

A Journal of the German Chemical Society

Angewandte

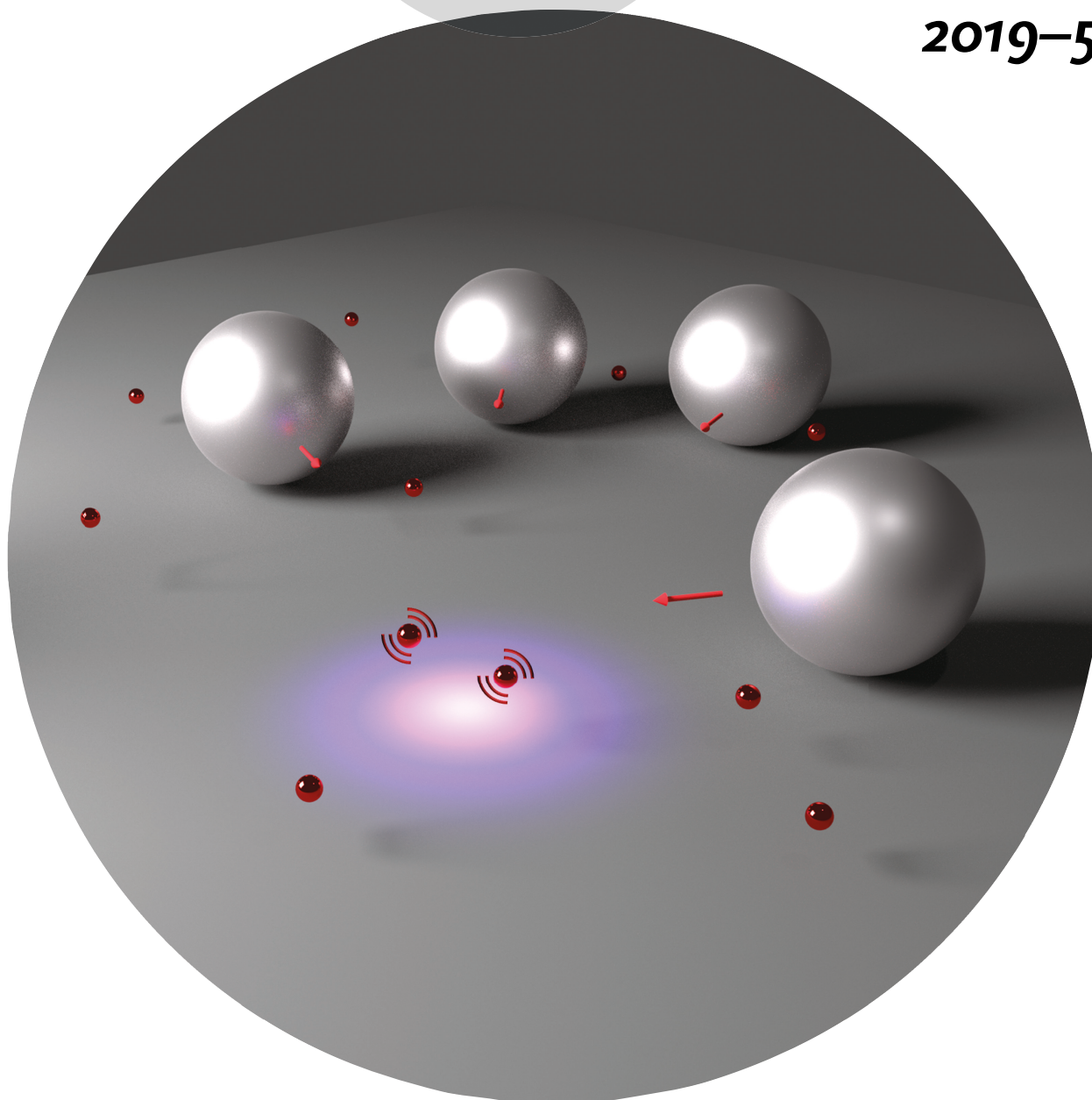
GDCh

Chemie

International Edition

www.angewandte.org

2019-58/8



The photothermal effect ...

... has been exploited to promote directional fluid pumping and inert particle assembly using suspensions of either gold or titanium dioxide nanoparticles. In their Communication on page 2295 ff., A. Sen, A. C. Balazs, and co-workers demonstrate the use of these directed flows to reversibly construct and move colloidal crystals. The cover picture is a schematic of gold nanoparticles being excited by UV light, which drives the assembly of larger micron-sized particles.

WILEY-VCH



Organization of Particle Islands through Light-Powered Fluid Pumping

Benjamin M. Tansi, Matthew L. Peris, Oleg E. Shklyaev, Anna C. Balazs,* and Ayusman Sen*

Abstract: The field of active matter holds promise for applications in particle assembly, cargo and drug delivery, and sensing. In pursuit of these capabilities, researchers have produced a suite of nanomotors, fluid pumps, and particle assembly strategies. Although promising, there are many challenges, especially for mechanisms that rely on chemical propulsion. One way to circumvent these issues is by the use of external energy sources. Herein, we propose a method of using freely suspended nanoparticles to generate fluid pumping towards desired point sources. The pumping rates are dependent on particle concentration and light intensity, making it highly controllable. Using these directed flows, we further demonstrate the ability to reversibly construct and move colloidal crystals.

The field of synthetic active matter was initiated by the findings of Paxton et al. in 2004.^[1] The authors constructed a bimetallic nanorod that could autonomously propel itself through solution by asymmetrically breaking down a chemical fuel. Since then, many examples of “motors” have been reported.^[2–5] When motors are affixed to a surface, they propel the surrounding fluid, in essence acting as a fluidic micropump.^[6] This in turn has led to the development of a host of reaction-based pumping systems featuring different materials and mechanisms.^[6–8] Such approaches eventually encompassed biology through the clever usage of enzyme molecules to yield pumping.^[9] However, the use of external energy sources has the added benefit of selective initiation and termination without needing to directly contact the system. Particularly attractive is the use of light as the external energy source owing to its ease of application and a high degree of control. Because of these advantages, the field of optofluidics has recently gained traction. Some studies have focused on the ability of metal patches to generate heat, but these require complex fabrication procedures.^[10,11] Herein, a method is presented to attain comparable control over fluid pumping without the need for prefabrication or preassembly of any kind.

For materials irradiated with light, a transduction between optical and mechanical energy can occur through an opto-

chemical or opto-thermal route. Notably, metallic catalysts can participate in both these mechanisms. With respect to the opto-chemical transduction, the high photocatalytic activity of titanium dioxide (TiO_2), which absorbs strongly in the ultraviolet region, enables TiO_2 microparticles to drive oxidation-reduction reactions and thereby undergo self-propulsion.^[12,13] This motion can occur through diffusiophoresis, which arises in response to a non-uniform distribution of ionic products around the particles. In addition to promoting photocatalytic activity, the absorbed optical energy is transduced into heat around the irradiated particles. Govorov et al. noted the existence of fluid flows when a suspension of gold nanoparticles were irradiated using a laser at their plasmon resonance wavelength.^[14] Beyond this finding, little attention has been paid to bulk fluid flows that are thermally activated by the irradiation of particles. To fill this gap, we examined the ability of TiO_2 microparticles, exposed to UV light, to generate thermally driven convective flows and harness this mechanism to assemble colloidal crystal monolayers. Such lattice structures are comprised of highly organized nano- and micron-scale particles and have gained attention owing to their potential in sensors, coatings, and optoelectronics.^[15,16] To provide a benchmark, we compare the behavior of the TiO_2 system to the well-studied heat generation by irradiated gold nanoparticles dispersed in an aqueous solution.^[17–20]

When a beam of ultraviolet light is focused on a suspension of titanium dioxide nanoparticles, the solution immediately begins to flow convectively about the region being irradiated. This was observed in a 1 cm-diameter steel-walled chamber with glass cover slips on the top and bottom (Supporting Information, Figure S1). The suspension was irradiated from below through a microscope objective (see the Supporting Information for details). The velocity of this fluid flow was observed to increase linearly with particle density. This is highlighted in Figure 1 A, in which the particle

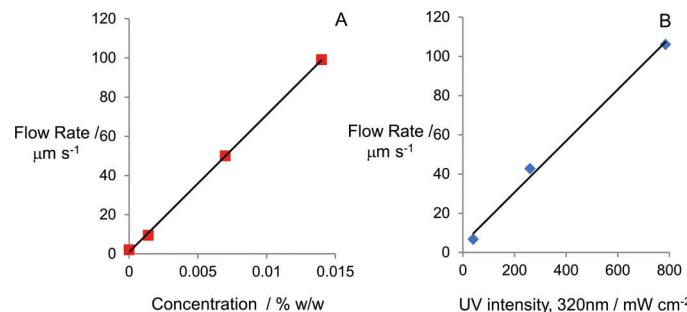


Figure 1. A) The flow rate towards the spot of UV irradiation as a function of weight percent of $360 \pm 70 \text{ nm}$ TiO_2 particles in water. Ten polystyrene tracer particles (10 μm) were tracked at each concentration. B) The flow rate also showed a linear dependence on UV light intensity. The standard deviation of each point was less than $3 \mu\text{m s}^{-1}$.

[*] B. M. Tansi, M. L. Peris, Dr. A. Sen

Department of Chemistry, Pennsylvania State University
University Park, PA 16802 (USA)
E-mail: asen@psu.edu

O. E. Shklyaev, Dr. A. C. Balazs
Department of Chemical Engineering, University of Pittsburgh
Pittsburgh, PA 15213 (USA)
E-mail: balazs@pitt.edu

Supporting information and the ORCID identification number(s) for the author(s) of this article can be found under:
<https://doi.org/10.1002/anie.201811568>.

density was varied up to 0.014% (w/v) of rutile powder in water. Similarly, it was seen that the pumping rate was dependent on the light intensity used to irradiate the sample (Figure 1B). These rates were all tested at the same height of 1140 μm above the bottom surface. By testing a series of different heights within the chamber, convection was observed in the form of inward pumping near the bottom of the chamber and outward pumping near the top. This is highlighted by the s-shaped curve given in Figure S2 (Videos 1 and 2). The lamp can be used to direct the location of the light spot and, therefore, the location of pumping. The convective nature of this fluid motion was further demonstrated using a glass-walled cell. When the bottom of the cell was irradiated with UV light, a thread-like strand of particles was ejected from the surface and proceeded to form convective rolls on either side of the irradiated region. This can be seen in Figure 2 and Video 3.

In order to demonstrate the utility of this technique, the induced flows were used to collect and organize assemblies of inert tracer particles. When the tracer particles (10 μm polystyrene beads) were allowed to settle out, the flows near the bottom surface carry the particles and organize them in the irradiated area. This can be used for the active particles themselves as well as for any tracer particles that are added to

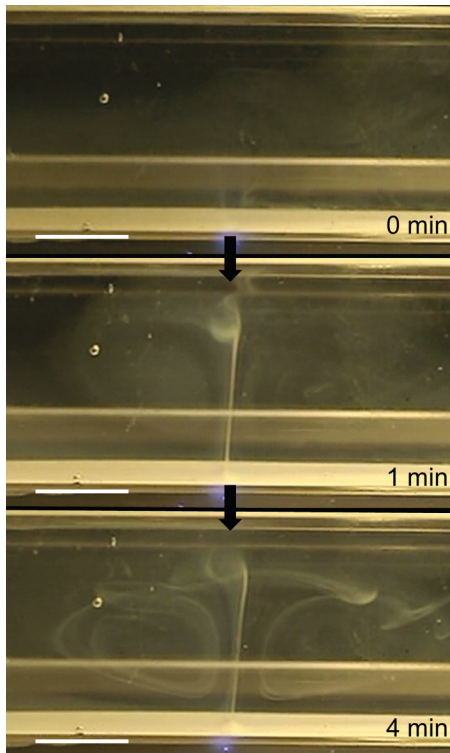


Figure 2. A flat-walled cell was used to visualize the convective flows arising from local particle heating. A 2 mg mL^{-1} $360 \pm 70 \text{ nm}$ TiO_2 particle suspension was allowed to settle out before being irradiated from below with ultraviolet light. The resulting fluid flows were strong enough to eject particles upwards as seen in the middle cell. This pumping proceeded to carry the particles through the characteristic loops of a bulk flow by convection. The chamber had a height of 1.2 cm and a width of 0.4 cm. It was cut to be 7 cm long. This process can be seen in Video 3. Scale bar = 0.5 cm.

the solution (Figure 3). When these inward flows are sustained for about 45 min to an hour, polystyrene tracer particles are pressed together into a two-dimensional close-packed architecture. This assembly was aided by the addition

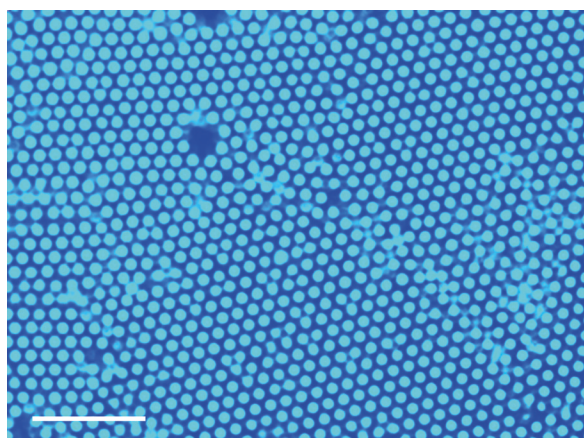


Figure 3. The ensemble of 10 μm polystyrene tracer particles will take on a close-packed arrangement owing to the uniform inward flow. The 10 μm polystyrene tracer particles demonstrate this packing while the solution is pumped by 0.007% w/w TiO_2 ($360 \pm 70 \text{ nm}$) in water (20 \times magnification). Sodium nitrate (0.14 mM) was added to mitigate buckling. This process can be seen in Video 4. Scale bar = 75 μm .

of sodium nitrate (0.14 mM) to mitigate buckling by increasing surface interactions. A demonstration of this is given in Video 4 in which the particles come together and then are pressed into the organized structure. Once the UV light is turned off, the particles immediately begin to diffuse randomly, slowly disassembling the colloidal crystal (Figure S3). If left overnight, the particles become dispersed across the bottom surface of the cell. At this point, they can be brought together again by irradiating a new region of the surface. In this way, we demonstrated the ability to reversibly collect particles anywhere within the sample chamber.

In addition to collecting in plane, the tracer particles will buckle if their concentration is sufficiently high. When the amount of tracers added was increased from 0.0064% w/v to 0.025% w/v, some of the particles were ejected from the monolayer as the ensemble was pressed together. In order to observe the height of the resulting mound, the cover was removed and water was allowed to evaporate while the sample was irradiated with UV light. By comparing the highest and lowest focal planes, it was seen that the 10 μm polystyrene tracers stacked to a height of 88 μm . This is detailed in section A2 of the Supporting Information. Dynamic assembly methods that provide 3D architectures are rare, making this a valuable first step towards future work in 3D nanoscale assembly.

The thermal convection mechanism was confirmed by varying the surface charges and ionic strength of the medium. Sodium nitrate was added to the suspension at a concentration of 214 mM. This raised the speed somewhat, but the direction remained the same (Figure S4). This rules out an ionic diffusiophoresis or electroosmotic mechanism for which the velocity should decrease with increasing ionic strength of the

medium.^[13,21] To supplement these results, cationic amino-polystyrene particles (6 μm , Polysciences) were used as tracers and the solution was adjusted to a pH value of 2 using hydrochloric acid. With the tracer particle zeta potential now increased to $18 \pm 6 \text{ mV}$ compared to $-50 \pm 3 \text{ mV}$ for the unfunctionalized particles, the direction of flow remained unchanged (Figure S4), again demonstrating that the observed fluid flows are charge independent.

Given the above results, follow-up experiments were performed using hexadecane as the medium in place of water. The titanium dioxide particles were found to aggregate significantly, and the addition of tracer particles was not necessary to observe the flows. Once again, inward flows were promoted upon UV irradiation. As with the above trials, the ability to pump under these conditions further indicates the charge and ion gradient independence of the pumping behavior. At a TiO_2 concentration of 0.007% w/v, flows were observed at $29 \pm 3 \text{ }\mu\text{m s}^{-1}$ as opposed to the $50 \pm 3 \text{ }\mu\text{m s}^{-1}$ observed in water (Figure S4). This decrease is attributed to the difference in viscosity between the two solvents. At 298.15 K, hexadecane has a dynamic viscosity of over three times that of water at 3.01 MPa s and 0.89 MPa s, respectively. To our knowledge this is the first demonstration of light-driven fluid pumping in an organic medium.

For comparison to these active particle suspensions, a patch of TiO_2 was fabricated and tested for its ability to generate flows. When UV light was directed towards the cell and away from the patch, flows were not observed. The light was then shifted over to the patch and flows immediately began in the region being irradiated. This is shown in Video 5. The patch was 100 nm thick, suggesting that even thin layers were sufficient to generate pumping at a modest rate.

To confirm that the particles were generating heat, a k-type thermocouple was inserted in the solution during UV irradiation. After increasing rapidly, a sustained temperature increase of 0.6–0.8 K was observed for TiO_2 (0.014% w/v, $360 \pm 70 \text{ nm}$; Figure S5). Since the pumping is attributed to local heating, it is important to note that this migration is not due to thermophoresis. First, the Soret constant is usually positive, indicating that particles would move from the hot towards the cold regions.^[11,12] The inward flows near the bottom would therefore be unexpected. The bulk fluid flow is also contrary to thermophoretic motion.

Gold nanoparticles ($21 \pm 5 \text{ nm}$) were also found to work well in promoting light-powered fluid flows (Figure S6). It is known that such particles in water will heat by about 5 K when irradiated at their plasmon resonance wavelength.^[22] This heat energy rapidly dissipates into the surrounding solution. In our system, a flow rate of $179 \text{ }\mu\text{m s}^{-1}$ is reached at 0.0001% w/v of gold in solution. By comparison, 0.014% w/v TiO_2 ($360 \pm 70 \text{ nm}$) yielded a flow rate of about $100 \text{ }\mu\text{m s}^{-1}$. This gold nanoparticle-based pumping system also demonstrates an increase in pumping rate with increasing particle concentration (Figure S6). On account of its much lower rate of aggregation, gold can be used to promote migration of tracer particle assemblies. When the irradiated region was shifted, the ensemble collectively migrated to the new location. An example of this is given in Figure 4 (Video 6). Large sections of the ensemble retain their colloidal crystal

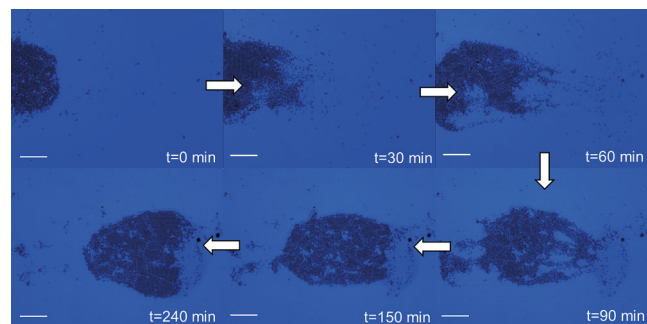


Figure 4. Migration of tracer particle ($10 \mu\text{m}$ PS) cluster owing to flows produced by heating gold nanoparticles ($21 \pm 5 \text{ nm}$). The ensemble of tracer particles was allowed to gather before the light was aimed elsewhere in the chamber. The light source and the window were moved to the right of where the particles were initially gathered (seen at left in the first frame). The light was shifted to the right by about $1500 \mu\text{m}$ and the particles were seen to move towards the new location. The images are arranged clockwise from top-left (5 \times magnification). Scale bar = 200 μm . Also shown in Video 6.

architecture as this transition occurs, while grain boundaries will form and anneal within the lattice structure.

To verify that the thermal buoyancy mechanism is responsible for the experimental observations, we developed a computational model for the corresponding system. As detailed in the Supporting Information, we consider a rectangular chamber (Figure 5) which contains an aqueous solution of uniformly dispersed gold particles with radius $r_p = 10.5 \text{ nm}$. Due to the particles' small radii, the sedimentation can be ignored and the particles are treated as a continuous field of a solute, with a uniform constant concentration C (particles m^{-3}), which is known from the experiment. When irradiated with UV light, the solution within the radius of the light beam, $R_l = 1 \text{ mm}$, begins to heat up. In particular, each gold particle in this region absorbs light and generates an amount of heat $q = 1.39 \text{ pW}$, calculated using the Mie theory for the case when r_p is much smaller than the wavelength of the light.^[23] A solution with a concentration C of particles generates a maximum total amount of heat $Q = qC$ (W m^{-3}). To describe the spatial distribution of the irradiated particles, we introduce a function f , which equals one when the particles are located within the region exposed to the light beam and zero otherwise. Then, the distribution of the heat sources in the solution is $Qf(r)$.

The dynamics of the non-uniformly heated fluid were modeled by solving the continuity, Navier–Stokes, and heat conduction equations with the source term $Qf(r)$. The heat absorbed from the UV light by the metallic particles is transferred to the solution and thus, gives rise to the buoyancy force, $g\rho_0\beta\Delta T$, which is proportional to gravity g , solvent density ρ_0 , thermal expansion coefficients $\beta = \partial\rho/\partial T$ and the temperature difference, ΔT , with respect to a reference value. Simulations presented in Figure 5 show how the fluid in the region irradiated by the UV light (orange circle) heats up and produces convective vortices, which aggregate polystyrene tracers into clusters that are centered on the spot heated by light and located at the bottom wall. When the source of light is shifted, the tracers follow and assemble at the new position.

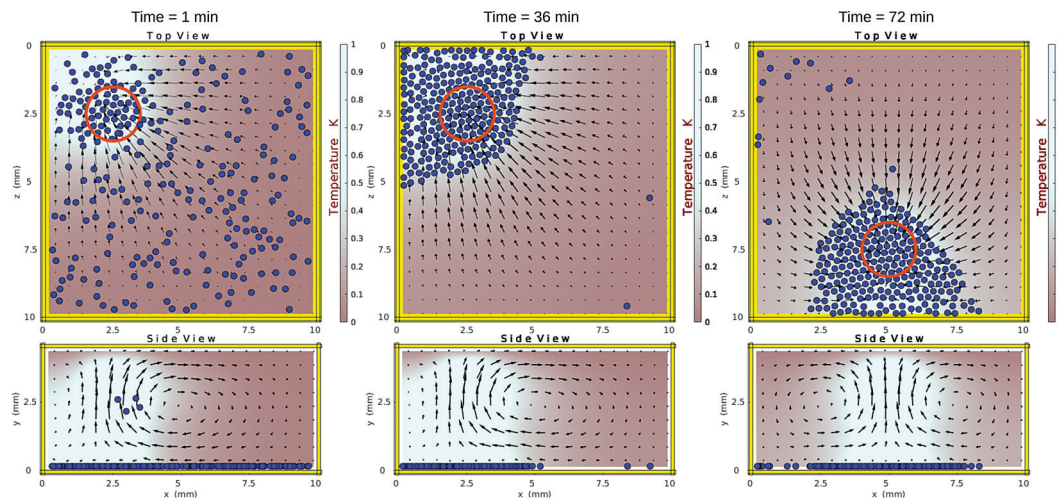


Figure 5. Aggregation of the tracer particles (blue spheres) induced by the heating of the aqueous solution of gold nanoparticles ($C=0.005\text{ \% w/w}$) by the UV light (red circle). The temperature ΔT (K) distribution is shown with a color-bar. The direction of the fluid velocities is indicated with black arrows. The left and middle panels show sequential stages of the aggregation by the UV light fixed at the position $x=z=2.5\text{ mm}$. The right panel shows the aggregated state induced by the UV light shifted to $x=5$ and $z=7.5\text{ mm}$. See the Supporting Information for additional figures and video.

The magnitude of the simulated flow velocities (Figure S9) is comparable to the experimental observation presented in Figure 1A and increases in a manner roughly proportional to the concentration of the metallic particles. The simulated structures of the aggregated clusters of tracers, shown in Figure S10, are qualitatively similar to the close-packed arrangement displayed in Figure 3.

In conclusion, we have demonstrated a method of producing highly controllable flows that can be utilized to collect particles around a point source. TiO_2 and gold particles serve as models for the technique, which can be performed without any preassembly, requiring only that care be taken in monitoring either the light intensity or the light-active particle concentration. The ability to locally concentrate inactive tracers can extend across many different media, easily gathering plastic particles. By using this method, one should be able to concentrate bacteria and other cells with the same level of ease. This technique can be used in any medium that does not react with the active particle or under UV irradiation. For the above reasons, this particle-based, light-driven flow technique is a powerful new addition to the toolbox of active matter-induced dynamic assembly strategies.

Acknowledgements

The authors would like to thank the Materials Research Institute at Penn State for the use of their facilities and for their useful insight. We also thank Josh Kauffman and Subhadip Ghosh for collecting SEM data and providing gold particles, respectively. This work was made possible by NSF-CCI Award Number 1740630.

Conflict of interest

The authors declare no conflict of interest.

Keywords: colloids · micropumps · nanoparticles · self-assembly · titanium dioxide

How to cite: *Angew. Chem. Int. Ed.* **2019**, *58*, 2295–2299
Angew. Chem. **2019**, *131*, 2317–2321

- [1] W. F. Paxton, K. C. Kistler, C. C. Olmeda, A. Sen, S. K. St. Angelo, Y. Cao, T. E. Mallouk, P. E. Lammert, V. H. Crespi, *J. Am. Chem. Soc.* **2004**, *126*, 13424–13431.
- [2] S. Sánchez, L. Soler, J. Katuri, *Angew. Chem. Int. Ed.* **2015**, *54*, 1414–1444; *Angew. Chem.* **2015**, *127*, 1432–1464.
- [3] F. Wong, K. K. Dey, A. Sen, *Annu. Rev. Mater. Res.* **2016**, *46*, 407–432.
- [4] P. Illien, R. Goleshtanian, A. Sen, *Chem. Soc. Rev.* **2017**, *46*, 5508–5518.
- [5] Y. Tu, F. Peng, D. A. Wilson, *Adv. Mater.* **2017**, *29*, 1–20.
- [6] C. Zhou, H. Zhang, Z. Li, W. Wang, *Lab Chip* **2016**, *16*, 1797–1811.
- [7] F. Wong, A. Sen, *ACS Nano* **2016**, *10*, 7172–7179.
- [8] S. Das, O. E. Shklyaev, A. Altemose, H. Shum, I. Ortiz-Rivera, L. Valdez, T. E. Mallouk, A. C. Balazs, A. Sen, *Nat. Commun.* **2017**, *8*, 1–10.
- [9] S. Sengupta, D. Patra, I. Ortiz-Rivera, A. Agrawal, S. Shklyaev, K. K. Dey, U. Córdova-Figueroa, T. E. Mallouk, A. Sen, *Nat. Chem.* **2014**, *6*, 415–422.
- [10] M. Li, Y. Su, H. Zhang, B. Dong, *Nano Res.* **2018**, *11*, 1810–1821.
- [11] J. S. Donner, G. Baffou, D. McCloskey, R. Quidant, *ACS Nano* **2011**, *5*, 5457–5462.
- [12] D. P. Singh, U. Choudhury, P. Fischer, A. G. Mark, *Adv. Mater.* **2017**, *29*, 1–7.
- [13] Y. Hong, M. Diaz, U. M. Córdova-Figueroa, A. Sen, *Adv. Funct. Mater.* **2010**, *20*, 1568–1576.
- [14] M. T. Carlson, T. S. Barton, P. J. Tandler, H. H. Richardson, A. O. Govorov, *MRS Proc.* **2009**, *1172*, 1172-T05-08.
- [15] B. J. Zhang, Y. Li, X. Zhang, B. Yang, *Adv. Mater.* **2010**, *22*, 4249–4269.

[16] B. O. D. Velev, E. W. Kaler, *Adv. Mater.* **2000**, *12*, 531–534.

[17] N. M. Dimitriou, G. Tsekenis, E. C. Balanikas, A. Pavlopoulou, M. Mitsogianni, T. Mantso, G. Pashos, A. G. Boudouvis, I. N. Lykakis, G. Tsigaridas, et al., *Pharmacol. Ther.* **2017**, *178*, 1–17.

[18] K. M. Haas, B. J. Lear, *Chem. Sci.* **2015**, *6*, 6462–6467.

[19] X. Huang, M. A. El-Sayed, *J. Adv. Res.* **2010**, *1*, 13–28.

[20] M. L. Brongersma, N. J. Halas, P. Nordlander, *Nat. Nanotechnol.* **2015**, *10*, 25–34.

[21] T. R. Kline, W. F. Paxton, Y. Wang, D. Velezol, T. E. Mallouk, A. Sen, *J. Am. Chem. Soc.* **2005**, *127*, 17150–17151.

[22] A. O. Govorov, W. Zhang, T. Skeini, H. Richardson, J. Lee, N. A. Kotov, *Nanoscale Res. Lett.* **2006**, *1*, 84–90.

[23] C. F. Bohren, D. R. Huffman, *Absorption and Scattering of Light by Small Particles*, Wiley-VCH, Weinheim, **1998**.

Manuscript received: October 8, 2018

Revised manuscript received: December 11, 2018

Accepted manuscript online: December 13, 2018

Version of record online: January 25, 2019